

Upwind Iteration Methods for the Cell Vertex Scheme in One Dimension

K. W. MORTON, M. A. RUDGYARD,* AND G. J. SHAW†

Oxford University Computing Laboratory, Numerical Analysis Group, 11 Keble Road, Oxford, England OX1 3QD

Received July 26, 1993

This paper describes and analyses a series of methods for solving the algebraic equations obtained from the cell vertex finite volume discretisation in one dimension. The objective is to explore the possibilities for improved iteration methods that may be applied to cell vertex discretisations of the Navier–Stokes equations in higher dimensions. In general there is no natural one-to-one correspondence between cell-based residuals and nodal unknowns for this system. In order to devise iteration schemes it is therefore necessary to provide a mapping between cells and nodes. The family of methods introduced here is based on the application of standard iterative techniques to a nodal residual formed of a combination of neighbouring cell-based residuals. It includes the familiar Lax–Wendroff iteration, upwind iteration schemes, and marching schemes capable of attaining convergence rates independent of the number of algebraic equations. The aim in each case is to set to zero the residual for each cell, apart from exceptional cells such as those containing shocks. The final results show that matrix-based upwind iteration methods, using cell residuals modified to take account of critical points and applying several local iterations, converge in around 15 iterations. © 1994 Academic Press, Inc.

1. INTRODUCTION

Most work on the iterative solution of algebraic systems arising from discretising differential equations relies on a basic diagonal dominance. For predominantly elliptic problems, on which the most effort has been concentrated, this usually arises naturally whether finite difference, element, or volume methods are used; and for convection-dominated flow problems it is common to force the issue by adding artificial dissipation to centrally differenced convective terms.

The cell vertex approach is different in several ways and gives no natural diagonal dominance. In a convection–diffusion problem it takes as its primary goal the accurate approximation of the convective terms; in one dimension this gives a two-point stencil, centred on a cell or interval

rather than a node, to which is added a four-point approximation to the diffusion, similarly centred. As shown, for example, in [4, 8, 11], such a scheme has many desirable approximation properties which are achieved without the need for adjusting any parameters as the balance between convection and diffusion changes. Thus the scheme is ideally suited to approximating the singularly perturbed equations of fluid dynamics at high Reynolds numbers. The emphasis is on the inviscid first-order terms, which yield steady equations of mixed hyperbolic/elliptic type even in subsonic regions and which are wholly hyperbolic in supersonic regions.

This approach is not, however, without its difficulties. Most importantly, there is not, in general, any natural one-to-one correspondence between discrete equations and unknowns. The lack of diagonal dominance is one consequence and the difficulty in constructing a general error analysis is another. This situation is usually circumvented by introducing a mapping between cells and nodes, which combines neighbouring cell residuals to produce a nodal residual. This nodal residual is then driven to zero by iteration, although fast convergence, and in particular mesh independent convergence, is often difficult to achieve. Moreover, this does not always ensure that the individual cell residuals are themselves set to zero, and indeed this is not always possible or desirable, for example, at shocks. As a result, a basically simple and attractive idea, which many researchers have considered, becomes progressively more complicated and, hence, is often abandoned.

This paper considers these issues in detail for typical one-dimensional problems. The aim is to take the cell vertex method as it has been developed and used successfully for multidimensional Navier–Stokes calculations in [1–3, 13], specialise it to one-dimensional problems where the convergence problems become apparent, and then explore possible means of remedying the situation by better definitions of the nodal residuals and improved iteration procedures. Sometimes it will be clear that these improvements, which can be very substantial, can be carried back to the multidimensional codes in a straightforward manner. More often further research will be needed to accomplish this, and

* Present address: CERFACS, 42, Avenue Gustave Coriolis, 31057 Toulouse Cedex, France.

† Present address: NAG Ltd, Wilkinson House, Jordan Hill Road, Oxford OX2 8DR, England.

the main value of the one-dimensional studies will be to provide a target for which to strive.

The layout of the paper is as follows. Sections 2 and 3 describe model problems and their discretisation by the cell vertex method. Section 4 introduces some simple marching schemes based on the application of the symmetric Gauss-Seidel iteration to a system of discrete nodal equations. These methods are shown to have a convergence rate that is independent of the number of unknowns for subcritical nozzle flow. Section 5 is devoted to the Lax-Wendroff method as an iteration scheme and its various generalisations; a convergence analysis based on the energy method is given and results presented for model problems which confirm the rôles of the various parameters involved. In Section 6 it is shown how various mappings between the cell-based residuals and nodal equations lead to general upwind iteration schemes which link the Lax-Wendroff method to the earlier simple marching scheme and solve the discrete equations in a number of steps that is independent of the number of cells. For the transonic nozzle flow problem, the ideal scheme involves splitting a residual in the sonic cell and combining two at the shock point. Finally, in the concluding section there is some speculation on the prospects of transferring the advances made in one dimension to multidimensional codes.

2. MODEL PROBLEMS

Consider an initial boundary value problem for the nonlinear system of m equations

$$\frac{\partial \mathbf{w}}{\partial t} + \frac{\partial \mathbf{f}}{\partial x} = \mathbf{g}, \quad x \in (x_L, x_R), \quad t \geq 0. \quad (2.1)$$

Here $\mathbf{f}(\mathbf{w})$ is normally a vector function of the m -vector of conserved variables $\mathbf{w}(x, t)$, and our main interest is in solving the steady problem

$$\frac{d\mathbf{f}}{dx} = \mathbf{g}, \quad x \in (x_L, x_R). \quad (2.2)$$

However, we may need to refer to the unsteady problem to resolve questions of nonuniqueness by consideration of solution stability; and since we wish that any methods developed for the Euler equations can be extended to the Navier-Stokes equations, we shall on occasion consider $\mathbf{f} = \mathbf{f}(\mathbf{w}, \mathbf{w}_x)$ to be a function of the gradient of the conserved variables, which also provides an alternative means of resolving nonuniqueness.

An example of such a system which will occur frequently

in the paper is one-dimensional nozzle flow, modelled by the isenthalpic Euler equations,

$$\mathbf{w} = \begin{pmatrix} \rho \\ \rho u \end{pmatrix}, \quad \mathbf{f} = \begin{pmatrix} \rho u \\ \rho u^2 + p \end{pmatrix}, \quad \mathbf{g} = \begin{pmatrix} 0 \\ (p/\sigma) d\sigma/dx \end{pmatrix}, \quad (2.3)$$

where ρ and p denote the density and pressure multiplied by the cross-sectional area σ of the nozzle and u is the velocity. The system is closed by the equation of state for an ideal gas which, with the constancy of the enthalpy, gives the pressure through the relations

$$p = \rho c^2/\gamma, \quad c^2 = [1 - \frac{1}{2}(\gamma - 1)u^2], \quad (2.4)$$

where γ is the ratio of specific heats for the gas. For subsonic inflow or outflow one boundary value should be prescribed. For supersonic inflow both values must be given, whilst no boundary data is required at a supersonic outflow. This problem has the analytical solution

$$\rho u = \mu, \quad \rho^{\gamma+1} = \nu \sigma^{\gamma-1} [\rho^2 - \frac{1}{2}(\gamma - 1)\mu^2], \quad (2.5)$$

where μ and ν are arbitrary constants determined by the boundary data. This solution is valid everywhere except at shocks, through which the values of the constants change according to the Rankine-Hugoniot relations; see, for example, [10] for details. Throughout this paper the cross-sectional area of the nozzle on the interval $-1 \leq x \leq 1$ is taken as

$$\sigma(x) = \pi [1 - \frac{1}{10}(1 + \cos \pi x)]^2. \quad (2.6)$$

We shall also refer on occasion to the linear convection-diffusion equation in the form

$$-\varepsilon \frac{d^2 w}{dx^2} + \frac{d}{dx}(aw) = g, \quad x \in (0, 1), \quad (2.7)$$

with Dirichlet boundary conditions at each end, $w(0) = w_L$ and $w(1) = w_R$ given; here ε is a small positive constant and $a(x)$, $g(x)$ are given functions.

Very often the finite interval on which a problem is posed is an approximation to an infinite interval. Then the boundary conditions may be given in terms of a state at infinity \mathbf{w}_∞ ; or, in the case where the system is dissipative, there may be states $\mathbf{w}_{-\infty}$ and \mathbf{w}_∞ at the left and right ends.

3. THE CELL VERTEX METHOD

We begin by considering the problem (2.2). Let the finite interval $[x_L, x_R]$ be divided by the points $x_L = x_0 <$

$x_1 < \dots < x_N = x_R$ into N subintervals. Suppose first that $\mathbf{g} = \mathbf{g}(x)$ so that (2.2) can be integrated exactly over each of these subintervals; if the total number of boundary conditions at the two ends of the interval is equal to m , then exact nodal values of \mathbf{f} can be obtained by solving a discrete system of $m(N+1)$ algebraic equations; and if $\mathbf{f}(\mathbf{w})$ has properties to ensure that it uniquely determines \mathbf{w} , the exact nodal solution is obtained.

This simple situation is not typical. More often $\mathbf{g} = \mathbf{g}(x, \mathbf{w})$ and, furthermore, the Jacobian $A(\mathbf{w}) = \partial \mathbf{f} / \partial \mathbf{w}$ has points of singularity. In general the integration over a cell cannot be performed exactly, but it is approximated using the trapezoidal rule to give

$$\begin{aligned} & \mathbf{f}(\mathbf{w}(x_j)) - \mathbf{f}(\mathbf{w}(x_{j-1})) \\ &= \int_{x_{j-1}}^{x_j} \mathbf{g}(s, \mathbf{w}(s)) ds \\ &\approx \frac{1}{2} h_{j-1/2} [\mathbf{g}(x_j, \mathbf{w}(x_j)) + \mathbf{g}(x_{j-1}, \mathbf{w}(x_{j-1}))], \end{aligned} \quad (3.1)$$

where $h_{j-1/2} = x_j - x_{j-1}$. The cell vertex approximation (2.2) is then based on

$$\begin{aligned} \mathbf{R}_{j-1/2}(\mathbf{W}_{j-1}, \mathbf{W}_j) &:= \frac{\Delta \mathbf{f}_{j-1/2}}{h_{j-1/2}} - \mu \mathbf{g}_{j-1/2} \\ &= \mathbf{0}, \quad 1 \leq j \leq N, \end{aligned} \quad (3.2)$$

where \mathbf{W}_j is an approximation to $\mathbf{w}(x_j)$, $\mathbf{f}_j = \mathbf{f}(\mathbf{W}_j)$, $\mathbf{g}_j = \mathbf{g}(x_j, \mathbf{W}_j)$, and $\Delta \cdot_{j-1/2}$, $\mu \cdot_{j-1/2}$ are respectively difference and averaging operators for the cell $[j-1, j]$.

Replacing the discrete solution in (3.2) by the true solution gives the truncation error; when the solution is smooth we may use Taylor expansions about the mid-point of the cell to obtain

$$\begin{aligned} \mathbf{R}_{j-1/2}(\mathbf{w}_{j-1}, \mathbf{w}_j) &= \left(\frac{\partial \mathbf{f}}{\partial x} - \mathbf{g} \right)_{j-1/2} \\ &+ \frac{1}{8} h_{j-1/2}^2 \left(\frac{1}{3} \frac{\partial^3 \mathbf{f}}{\partial x^3} - \frac{\partial^2 \mathbf{g}}{\partial x^2} \right)_{j-1/2} \\ &+ O(h_{j-1/2}^4). \end{aligned} \quad (3.3)$$

If each residual (3.2) can be set to zero, we therefore expect that the approximation $\{\mathbf{W}_j\}$ is second-order accurate in smooth flow regions and that this is true regardless of the mesh variation. However, we shall see that there are classes of problems for which we are unable to ensure that each residual is zero.

Consider a scalar model problem with conditions $W_0 = w_L$, $W_N = w_R$, and the flux Jacobian $a(w_L) > 0$ and $a(w_R) < 0$; we require the solution at $N+1$ grid points but have N residuals and two boundary conditions. Thus the

system is over-determined and the residuals will have to be combined in some way. By contrast, for solutions which possess a single transcritical expansion wave, with $a(w_L) \leq 0$ and $a(w_R) \geq 0$, no boundary conditions are imposed and the result is an undetermined system and the possibility of multiple discrete solutions. This is a difficult case with many complications: in the example $(\partial w / \partial t + a(w) \partial w / \partial x) = g(x)$, a smooth steady solution exists only if g is zero at some point $x = x_c$ and $w(x_c) = \bar{w}$, where $a(\bar{w}) = 0$, but it is still difficult to integrate the equation from this critical point. If an iterative solution is attempted, it models the unsteady problem (which is always well posed) but even if it converges, the result obtained may depend on the details of the algorithm used and the initial conditions. As discussed below, the preferred resolution of the counting problem in one dimension is to create an extra equation by recovering the position of the critical point and splitting the residual there, which corresponds to using the local differentiated form $a'(\partial w / \partial x)^2 = g'$ to get out of the critical point; but the alternative of adding local dissipation is more generally applicable and just as effective.

The incorrect counting of equations and unknowns for the above problems is a direct consequence of the existence of critical points $a(w) = 0$ in the continuous solution. We may therefore expect difficulties to arise for systems of equations when an eigenvalue of the Jacobian matrix A passes through zero; this corresponds to the existence of sonic points and shock waves in the case of the steady Euler equations (2.3). If an iterative technique such as Lax-Wendroff is used in an attempt to solve the cell vertex equations, the treatment of these critical points is crucial to the quality of the converged solution.

To apply the cell vertex method to the second-order convection-diffusion equation (2.7), an approximation to the solution gradient at the nodes is needed. Instead of (3.2), the residual then becomes

$$\begin{aligned} R_{j-1/2}(W_{j-1}, W'_{j-1}; W_j, W'_j) \\ := \frac{1}{h_{j-1/2}} \left[\Delta(-\varepsilon W' + aW)_{j-1/2} - \int_{x_{j-1}}^{x_j} g(s) ds \right]. \end{aligned} \quad (3.4)$$

The second-order accurate approximation to W'_j that is used in [11] is

$$\begin{aligned} W'_j := \frac{1}{h_{j-1/2} + h_{j+1/2}} \left[h_{j-1/2} \frac{\Delta W_{j+1/2}}{h_{j+1/2}} + h_{j+1/2} \frac{\Delta W_{j-1/2}}{h_{j-1/2}} \right], \\ 1 \leq j \leq N-1, \end{aligned} \quad (3.5)$$

with W'_0 defined by extrapolation,

$$\frac{1}{2} h_{1/2} (W'_0 + W'_1) = \Delta W_{1/2}. \quad (3.6)$$

We again have a counting problem, however; because of the

Dirichlet boundary condition imposed at each end of the interval, there are only $N - 1$ unknowns and a possible N residual equations. Mackenzie and Morton [11] show by detailed error analysis that in the case $a(x) > 0$ it is the last residual on the right that should be discarded so that the interior unknowns are given by

$$R_{j-1/2} = 0, \quad 1 \leq j \leq N - 1. \quad (3.7)$$

We shall be interested in iterative methods for the solution of the system (3.7), which has an unusual form, and for others which arise from combining residuals.

The definition of the cell residual in (3.4) is a direct specialisation of that used for the Navier–Stokes equations in [1]; but the solution procedure used there was based on a Lax–Wendroff combination of neighbouring residuals, application of artificial viscosity terms, and multigrid. We shall consider Lax–Wendroff in Section 5, but first we consider more direct means of solving systems of the form (3.2) and (3.7).

4. SIMPLE MARCHING SCHEMES

In this section we consider marching schemes for solving the individual nonlinear cell vertex equations (3.2) when the Jacobian A has eigenvalues of different signs. The section begins with a description of a particularly simple yet effective marching method, applied to subcritical isenthalpic nozzle flow. This is then generalised to a partially successful scheme for the transonic nozzle problem. There follows some analysis of the scheme which gives some guidelines for the choice of distribution matrices, but also indicates some of the limitations of the approach.

4.1. A Marching Scheme for Subsonic Nozzle Flow

For the isenthalpic Euler equations (2.3) there are two residuals that may be set to zero in each cell:

$$R_{j-1/2}^{(1)} := \frac{(\rho u)_j - (\rho u)_{j-1}}{h_{j-1/2}} \quad (4.1)$$

and

$$R_{j-1/2}^{(2)} := \frac{(\rho u^2 + p)_j - (\rho u^2 + p)_{j-1}}{h_{j-1/2}} - \frac{1}{2} \left[\left(\frac{p}{\sigma} \frac{d\sigma}{dx} \right)_{j-1} + \left(\frac{p}{\sigma} \frac{d\sigma}{dx} \right)_j \right], \quad (4.2)$$

with p defined by the equation of state (2.4) and the nozzle shape σ given by (2.6). For subcritical flow the system will

normally have one boundary condition at inflow and one at outflow. Let these boundary conditions be denoted

$$B_0(\mathbf{W}_0) = 0, \quad B_N(\mathbf{W}_N) = 0. \quad (4.3)$$

A simple marching scheme which we shall generalise in the next section proceeds in the following way. The nodes of the mesh are scanned first from left to right and then in reverse order. At each interior node the state vector \mathbf{W}_j is updated by applying η iterations of Newton’s method to the nonlinear system comprising $R_{j-1/2}^{(1)} = 0$ and $R_{j+1/2}^{(2)} = 0$. At boundaries the undefined residual is replaced by the given boundary condition. This procedure is illustrated schematically by Fig. 1.

We consider the behaviour of this method for various choices of the boundary data. Suppose that the pressure is given at outflow. Thus

$$B_N(\mathbf{W}_N) := p_N - p_\infty. \quad (4.4)$$

It is not difficult to see that if the momentum is defined at inflow and the local nonlinear equations are solved exactly at each node, then the constant momentum is swept downstream to the outflow, where an exact state is obtained. This enables the return sweep to generate an exact solution of the discrete algebraic system. Hence the definition

$$B_0(\mathbf{W}_0) := (\rho u)_0 - (\rho u)_\infty, \quad (4.5)$$

together with a sufficiently large value of η leads to a direct method. The behaviour of this scheme for various values of η is shown in Table I(a), which shows the number of double sweeps required to reduce the discrete l_2 norm of the cell residuals to less than 10^{-9} , starting from a random perturbation of a constant state. The inlet Mach number was fixed at 0.4, leading to a purely subsonic flow. The table clearly shows that if η is chosen large enough, such that the local nonlinear problem is solved exactly, then the method requires only one double sweep and it is effectively direct.

The forward sweep transports some part of the inflow data directly to the outflow boundary, where the state vector is modified to be consistent with this transported data, together with the outflow data. The return sweep then returns some part of this state to the inflow. The speed of the transportation process is independent of the number of cells

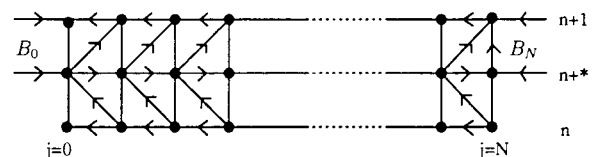


FIG. 1. Schematic diagram for marching scheme.

TABLE I

Number of Double Sweeps Needed for Convergence of Simple Marching Scheme with (a) Momentum and (b) Velocity Prescribed at Inflow

(a)					(b)				
<i>N</i>	$\eta=1$	$\eta=3$	$\eta=5$	$\eta=10$	<i>N</i>	$\eta=1$	$\eta=3$	$\eta=5$	$\eta=10$
17	6	2	2	1	17	*	19	19	19
33	7	2	2	1	33	*	20	19	19
65	9	3	2	1	65	*	20	19	19
129	12	3	2	1	129	*	*	20	20
257	15	3	2	1	257	*	*	20	20

Note. η is the number of Newton iterations at each node and * indicates a lack of convergence.

in the grid. Thus the convergence of the entire process depends only on the number of iterations required to resolve the two boundary states. This intuitive argument is confirmed by the results shown in Table I(b), for which the velocity is prescribed at inflow. Apart from a weak dependence of the required value of η on N , the method converges independently of the number of nodes. This convergence compares very favourably indeed with the results for Lax–Wendroff presented in Section 5.4.

4.2. A Generalisation for Transonic Flow

When the flow is wholly supersonic both residuals will be set to zero on the sweep from inflow to outflow. Thus in the transonic case we shall need to switch to this situation from that described above in Section 4.1. For this purpose we introduce a notation that we shall need later: for each cell we define matrices $D_{j-1/2}^{\pm}$; and then at each interior point we apply Newton’s method to the solution of the system

$$D_{j-1/2}^+ \mathbf{R}_{j-1/2} = 0 = D_{j+1/2}^- \mathbf{R}_{j+1/2}, \quad 1 \leq j \leq N-1. \quad (4.6)$$

As so far required these could be rectangular matrices which could be combined to give a simple $m \times m$ square matrix. However, to keep the notation consistent with that used for other schemes below, we shall fill out each matrix to a full $m \times m$ matrix and restrict its structure. For the purposes of this section, we shall assume for the pair of matrices in (4.6) that (i) there are no rows which are non-zero in both cases and (ii) that their sum is non-singular. We shall write this as

$$D_{j-1/2}^+ \overset{\text{(rows)}}{\cap} D_{j+1/2}^- = \emptyset, \quad \text{rank}(D_{j-1/2}^+ + D_{j+1/2}^-) = m, \quad 1 \leq j \leq N-1. \quad (4.7)$$

For example, in the simple scheme of Section 4.1 and for subsonic nodes in the present case, we have

$$D_{j-1/2}^+ = \begin{pmatrix} 1 & 0 \\ 0 & 0 \end{pmatrix}, \quad D_{j+1/2}^- = \begin{pmatrix} 0 & 0 \\ 0 & 1 \end{pmatrix}, \quad 1 \leq j \leq N, \quad (4.8)$$

which clearly satisfy these assumptions; for supersonic nodes $D_{j-1/2}^+$ is the identity matrix and $D_{j+1/2}^-$ is the null matrix.

Furthermore, we assume that the system to be solved at each boundary has the correct rank; thus we assume that the boundary conditions can be linearised with respect to the boundary fluxes to yield $m \times m$ square matrices D_0 and D_N for which similar properties hold:

$$D_0 \overset{\text{(rows)}}{\cap} D_{1/2}^- = \emptyset, \quad \text{rank}(D_0 + D_{1/2}^-) = m \quad (4.9a)$$

$$D_{N-1/2}^+ \overset{\text{(rows)}}{\cap} D_N = \emptyset, \quad \text{rank}(D_{N-1/2}^+ + D_N) = m. \quad (4.9b)$$

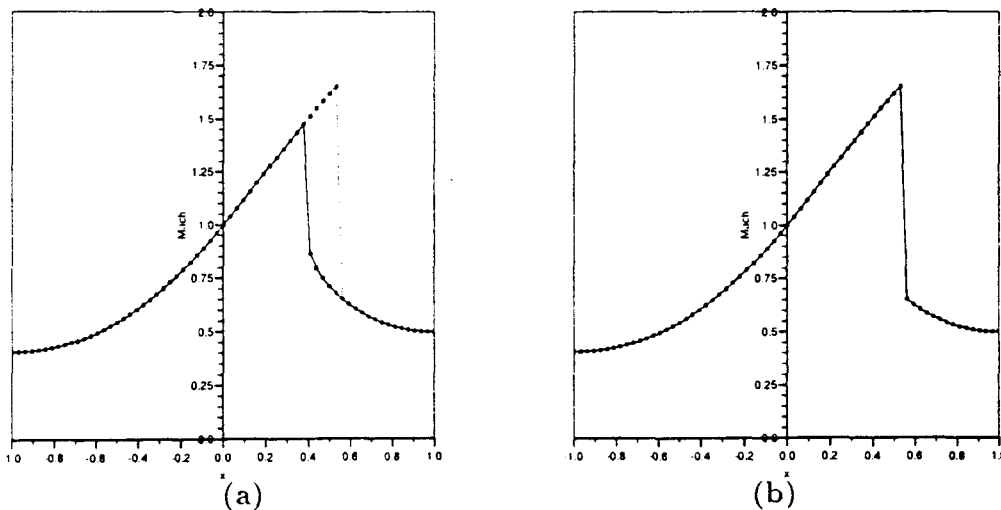


FIG. 2. Marching scheme for the transonic problem (a) without shock fitting and (b) after shock fitting; the exact solution is shown as a dotted line.

In Section 4.1 the inflow boundary condition can be interpreted as giving a D_0 which has only the first row non-zero and which is identical to the matrices $D_{j-1/2}^+$ when the momentum is prescribed but has two non-zero entries when the velocity is prescribed.

For nozzle flow with subsonic inflow and outflow, we suppose that a single interior supersonic region is possible. Then the marching algorithm described in Section 4.1 can be modified by either a preliminary scan to find this region or by finding it as part of the marching problem. In either case the sweep to the right begins as in the subsonic case, updating \mathbf{W}_j at all nodes until that on the left of the sonic cell is reached. At the sonic cell $R^{(2)}$ will be needed both to update the subsonic node on its left and the supersonic node on its right. This residual is therefore split at the predicted sonic point: interpolation of the Mach number defines the sonic point position and hence the state vector there and the partial residuals. So the subsonic partial residual $(R^{(2)})^-$ enables the final subsonic state vector to be updated, while the supersonic partial $(R^{(2)})^+$ enables the sweep through the supersonic cells to start. This can be continued right through to the node on the left of the shock cell; the whole sweep can then be completed through the subsonic nodes. The return sweep can be carried out in a similar manner either using the same sonic cell and shock cell locations or finding them dynamically.

However, this simple scheme cannot work satisfactorily. The location and treatment of a sonic cell is easy and effective; but the switch at a shock cell omits any use of the $R^{(2)}$ residual for that cell and so it cannot satisfy the global conservation law for the momentum. The result is an incorrectly positioned shock. One solution is to use shock fitting, by introducing the shock position as an internal boundary and a new state either side and then applying the Rankine–Hugoniot shock relations, as was done in two dimensions in [14]. This gives an effective overall scheme, as can be seen from the results of Fig. 2 which are for an inlet Mach number of 0.5; but it is too complicated for general adoption in multidimensions. Although simpler two-dimensional shock fitting procedures are given in [15], we shall find in the next two sections that there are much simpler procedures which are almost as effective. We shall see that the problem lies with the sudden switch in the distribution matrices at a shock, rather than being able to combine residuals from two cells at a node.

4.3. Analysis of the Marching Schemes for $\mathbf{f}_x = \mathbf{g}$

Suppose \mathbf{g} is a function of x only, so that in setting up the equations of \mathbf{W}_j we may assume that it is integrated exactly. Then writing the nodal error at iteration n as $\mathbf{E}_j^n := \mathbf{W}_j^n - \mathbf{w}(x_j)$ and allowing for two neighbouring nodes to be at different iterative stages, we will have

$$\begin{aligned} h_{j-1/2} \mathbf{R}_{j-1/2}^{n,m} &= [\mathbf{f}(\mathbf{W}_j^n) - \mathbf{f}(\mathbf{W}_{j-1}^m)] \\ &\quad - [\mathbf{f}(\mathbf{w}(x_j)) - \mathbf{f}(\mathbf{w}(x_{j-1}))] \\ &= A_j^n \mathbf{E}_j^n - A_{j-1}^m \mathbf{E}_{j-1}^m, \end{aligned} \quad (4.10)$$

for some set of matrices $\{A_j^n\}$, approximating the Jacobian matrices $\{\mathbf{A}(\mathbf{w}(x_j))\}$ when the $\{E_j^n\}$ are sufficiently small.

Similarly, suppose we can write the boundary conditions in the form

$$B_0^n \mathbf{E}_0^n := \mathbf{B}_0(\mathbf{W}_0^n) - \mathbf{B}_0(\mathbf{w}(x_L)) = 0 \quad (4.11a)$$

$$B_N^n \mathbf{E}_N^n := \mathbf{B}_N(\mathbf{W}_N^n) - \mathbf{B}_N(\mathbf{w}(x_R)) = 0 \quad (4.11b)$$

for some rectangular matrices B_0^n and B_N^n . Now consider the system that is solved for \mathbf{W}_0^n given \mathbf{W}_1^m and the boundary condition: it has the form

$$B_0^n \mathbf{E}_0^n = \mathbf{0}, \quad D_{1/2}^-(A_0^n \mathbf{E}_0^n - A_1^m \mathbf{E}_1^m) = 0. \quad (4.12)$$

We suppose this is solvable for \mathbf{E}_0^n and write its solution as

$$\mathbf{E}_0^n = C_{01}^n \mathbf{E}_1^m, \quad (4.13)$$

where we have written C_{01}^n to indicate that it depends on A_1^m as well as A_0^n . Similarly, on the right we have

$$B_N^n \mathbf{E}_N^n = \mathbf{0}, \quad D_{N-1/2}^+(A_N^n \mathbf{E}_N^n - A_{N-1}^m \mathbf{E}_{N-1}^m) = 0, \quad (4.14)$$

whose solution we rewrite as

$$\mathbf{E}_N^n = C_{N1}^n \mathbf{E}_{N-1}^m. \quad (4.15)$$

This puts us in the position of proving a convergence result for cases when the same distribution matrices are used throughout the problem domain, as with the subsonic nozzle.

THEOREM 4.1. *Assume that, in the problem $d\mathbf{f}/dx = \mathbf{g}$, \mathbf{g} is a function of x only, that the distribution matrices $D_{j-1/2}^\pm$ used in the marching process equal D^\pm independent of j and of n , and that the systems (4.12), (4.14) to be solved at the boundaries are uniquely solvable in the forms (4.13), (4.15). Then the convergence of the marching process is independent of the number of mesh points; and it depends only on the convergence of*

$$\mathbf{E}_0^n = (C_{0N}^n C_{N0}^n) \mathbf{E}_0^{n-1}, \quad (4.16)$$

for certain matrices C_{0N}^n and C_{N0}^n .

Proof. \mathbf{W}_0^n and, hence, \mathbf{E}_0^n are determined by solving the system at the left boundary, after the right to left sweep at the end of the n th iteration, from data $D^- A_1^n \mathbf{E}_1^n$ as in (4.12).

But in this sweep we have $D^- \mathbf{R}_{j+1/2}^{n,n} = \mathbf{0}$, $j = 1, 2, \dots, N-1$, where that is,

$$D^- A_1^n \mathbf{E}_1^n = D^- A_2^n \mathbf{E}_2^n = \dots = D^- A_N^n \mathbf{E}_N^n.$$

By the hypotheses of the theorem, the system formed from B_0^n and $D^- A_0^n$ can be solved for \mathbf{E}_0^n ; thus the solution depends on $A_N^n \mathbf{E}_N^n$ and we write it as

$$\mathbf{E}_0^n = C_{0N}^n \mathbf{E}_N^n. \quad (4.17)$$

Similarly, \mathbf{E}_N^n may be determined at the right boundary from the data $D^+ A_{N-1}^{n-1/2} \mathbf{E}_{N-1}^{n-1/2}$, where $\{\mathbf{E}^{n-1/2}\}$ denotes the set of values left at the intermediate stage after the left to right sweep during the n th iteration. But in this sweep we have $D^+ \mathbf{R}_{j-1/2}^{n,n-1} = \mathbf{0}$, $j = 1, 2, \dots, N-1$ so that

$$\begin{aligned} D^+ A_{N-1}^{n-1/2} \mathbf{E}_{N-1}^{n-1/2} &= D^+ A_{N-2}^{n-1/2} \mathbf{E}_{N-2}^{n-1/2} = \dots \\ &= D^+ A_0^{n-1/2} \mathbf{E}_0^{n-1/2} \end{aligned}$$

and $\mathbf{E}_0^{n-1/2}$ is the value \mathbf{E}_0^{n-1} left at the end of the previous iteration. Hence we write

$$\mathbf{E}_N^n = C_{N0}^n \mathbf{E}_0^n \quad (4.18)$$

so that (4.16) follows. ■

It is straightforward to generalise this result to cover the marching process used for subsonic nozzle flow in Section 4.1. The proper matching of the distribution matrices to the boundary conditions is clearly the key requirement for fast convergence. To exemplify this let us consider the equations linearised about a constant flow of unit density and velocity U . Then the equations and Jacobian are of the form

$$\begin{aligned} U\rho_x + u_x &= g_1, \\ c^2 \rho_x + Uu_x &= g_2, \end{aligned} \quad A = \begin{pmatrix} U & 1 \\ c^2 & U \end{pmatrix}, \quad (4.19)$$

where c is the sound speed. Suppose that u is given at inflow and ρ at outflow, while the equations to be solved at each internal node comprise a $(\theta^+ : 1 - \theta^+)$ weighted average of the residuals from the left and a $(\theta^- : 1 - \theta^-)$ average from the right; that is, the distribution matrices have the form

$$D^+ = \begin{pmatrix} 0 & 0 \\ \theta^+ & 1 - \theta^+ \end{pmatrix}, \quad D^- = \begin{pmatrix} \theta^- & 1 - \theta^- \\ 0 & 0 \end{pmatrix}. \quad (4.20)$$

Thus the equation system that is solved on the left gives, from (4.12),

$$C_0 = \begin{pmatrix} \alpha^- & \beta^- \\ 0 & 1 \end{pmatrix}^{-1} \begin{pmatrix} \alpha^- & \beta^- \\ 0 & 0 \end{pmatrix} = \begin{pmatrix} 1 & \beta^-/\alpha^- \\ 0 & 0 \end{pmatrix}, \quad (4.21a)$$

$$\alpha^- = \theta^- U + (1 - \theta^-) c^2, \quad \beta^- = \theta^- + (1 - \theta^-) U. \quad (4.21b)$$

Similarly, on the right we have from (4.14),

$$C_N = \begin{pmatrix} 1 & 0 \\ \alpha^+ & \beta^+ \end{pmatrix}^{-1} \begin{pmatrix} 0 & 0 \\ \alpha^+ & \beta^+ \end{pmatrix} = \begin{pmatrix} 0 & 0 \\ \alpha^+/\beta^+ & 1 \end{pmatrix}, \quad (4.22)$$

where α^+ and β^+ are defined as in (4.21b). Hence from (4.16) the convergence of the marching process is determined by the spectral radius of

$$C_0 C_N = \begin{pmatrix} \alpha^+ \beta^- / \alpha^- \beta^+ & \beta^- / \alpha^- \\ 0 & 0 \end{pmatrix}, \quad (4.23)$$

that is, by the ratio $\alpha^+ \beta^- / \alpha^- \beta^+$. In particular, for the choice used in Section 4.1, namely $\theta^+ = 1, \theta^- = 0$, the convergence factor is U^2/c^2 , which is less than one for the assumption of subsonic flow. Moreover, the observed data of Table I(b) correspond to an error reduction per double sweep of 0.355, which is in good agreement with this prediction for a problem where the Mach number lies in the range [0.4, 1.0].

Another important example, valid in the general linear case, is when each row of B_0 is a scalar multiple of a corresponding row of $D^+ A$. We may then show that the matrix $C_0 C_N$ is nilpotent of index two, regardless of the outflow boundary conditions, and we may use (4.16) to prove that $\mathbf{E}_0^2 = \mathbf{0}$. In fact, this convergence result is somewhat pessimistic, since $\mathbf{E}_0^1 = C_N C_0 \mathbf{E}_1^0$ and the matrix $C_N C_0$ is null under these conditions; this explains why we obtain convergence in one double sweep by taking the local iterations to convergence in Table I(a).

4.4. A Marching Scheme for Convection-Diffusion

The system of Eqs. (3.4)–(3.7), for which we have assumed that $a(x) > 0$, yields a matrix with a bandwidth of four elements. In general it is not obvious how best to solve this iteratively; but when convection is dominant, a marching scheme (from left to right) becomes a very natural approach. In calculating W_j^n , we have W_{j-1}^n and W_{j-2}^n but we need a value for W_j' ; the proposed approach is to calculate it from (3.5) using $\Delta W_{j-1/2}^n$ and $\Delta W_{j+1/2}^{n-1}$ from the previous iteration.

On a uniform mesh with constant a we define the mesh Péclet number as $\beta := ah/\varepsilon$. Then it is straightforward to show that this iteration will converge if $\beta > 1$, with an error reduction factor per iteration of $(2\beta - 1)^{-1}$. For

comparison, a direct application of a Gauss–Seidel iteration to the nodal equations converges if $\beta \geq \frac{1}{2}$; but for example at $\beta = \frac{3}{2}$, the convergence factor is at most $\frac{27}{40}$ rather than the value of $\frac{1}{2}$ given for the proposed scheme.

Convergence results can be derived on a non-uniform mesh and for a variable a , but as our main interest here is in the inviscid flow equations, these will be given elsewhere.

5. LAX–WENDROFF AS AN ITERATION METHOD

5.1. Formulation

Following Ni [16], the most common iteration schemes for the cell vertex discretisation are based on pseudo-time stepping using the Lax–Wendroff algorithm, in either the one-step or the two-step form. In this section we discuss its development, analysis, and application for a first-order system typified by our model problem (2.2) with $\mathbf{f} = \mathbf{f}(\mathbf{w})$. We use the notation $\delta \mathbf{W}$ for the update $\mathbf{W}^{n+1} - \mathbf{W}^n$ of the approximation, and the Taylor expansion on which the one-step form is based can be written in terms of the exact solution \mathbf{w} of the unsteady equation (2.1) as

$$\delta \mathbf{w} \approx -\Delta t \left\{ \frac{\partial \mathbf{f}}{\partial x} - \mathbf{g} \right\} + \frac{1}{2} \Delta t^2 \left\{ \frac{\partial}{\partial x} \left(A \left(\frac{\partial \mathbf{f}}{\partial x} - \mathbf{g} \right) - B_g \left(\frac{\partial \mathbf{f}}{\partial x} - \mathbf{g} \right) \right) \right\}, \quad (5.1)$$

where $B_g = \partial \mathbf{g} / \partial \mathbf{w}$ and Δt is a time step. In calculating $\delta \mathbf{W}$, cell residuals replace $(\partial \mathbf{f} / \partial x - \mathbf{g})$ in this expression and we clearly need to combine those from two neighbouring cells to update \mathbf{W} at the point between them.

The result can be written, with a local (nodal) time step, in the form

$$\delta \mathbf{W}_j = -\frac{\Delta t_j}{h_{j-1/2} + h_{j+1/2}} (D_{j-1/2}^+ h_{j-1/2} \mathbf{R}_{j-1/2} + D_{j+1/2}^- h_{j+1/2} \mathbf{R}_{j+1/2}), \quad (5.2)$$

where D^+ and D^- are distribution matrices which play a similar rôle to those in (4.6) and the residuals are given by (3.2). For a first-order update (i.e., neglecting the Δt^2 term in (5.1)) the two residuals should be combined so as to give a single residual over the pair of cells, thus not involving \mathbf{f}_j ; this corresponds to replacing D^+ and D^- by the identity matrix I , and the resulting $h_{j\pm 1/2}$ volume weighting of the residuals is important for convergence—see Hall [5] and Morton, Childs, and Rudgyard [12]. However, the negative definite term of the form $\delta(A^2 \delta \mathbf{W})$, provided by the second-order update is also necessary for convergence,

while the B_g term is relatively unimportant. So we take the Lax–Wendroff distribution matrices to be of the form

$$D_{j-1/2}^\pm = I \pm \frac{\bar{A}_{j-1/2} \Delta t_{j-1/2}}{h_{j-1/2}}, \quad (5.3)$$

where we have introduced further (cell-based) time steps $\Delta t_{j-1/2}$, and $\bar{A}_{j-1/2}$ is an average value of A for the cell. The resulting generalised Lax–Wendroff iteration was introduced in [12] for use with the Euler equations and has been applied very successfully by Crumpton, Mackenzie, and Morton [1] to the solution of the Navier–Stokes equations. The best choice of $\bar{A}_{j-1/2}$ is probably the Roe average but a simple practical choice is $A(\mu \mathbf{W})$.

This choice of distribution matrices has a conservation property which is important when one cannot ensure that all the cell residuals are set to zero after the iteration has converged.

LEMMA 5.1. *Suppose that for some constant matrix K*

$$D_{j-1/2}^+ + D_{j-1/2}^- = K \quad \forall j. \quad (5.4)$$

Then when the iteration (5.2) is applied for $j = 1, 2, \dots, N-1$ with any set of boundary conditions, convergence implies the conservation relations

$$\begin{aligned} & [K \mathbf{f}_{N-1} + D_{N-1/2}^-(\mathbf{f}_N - \mathbf{f}_{N-1})] - [K \mathbf{f}_1 - D_{1/2}^+(\mathbf{f}_1 - \mathbf{f}_0)] \\ &= D_{1/2}^+ h_{1/2} \mu \mathbf{g}_{1/2} + D_{N-1/2}^- h_{N-1/2} \mu \mathbf{g}_{N-1/2} \\ &+ K \sum_1^{N-2} h_{j+1/2} \mu \mathbf{g}_{j+1/2}. \end{aligned} \quad (5.5)$$

Proof. Multiply (5.2) by the node-based ratio $(h_{j-1/2} + h_{j+1/2}) / \Delta t_j$ and sum over j . When $\delta \mathbf{W}_j \rightarrow 0 \forall j$ the sum is zero and collapses to (5.5). ■

Satisfaction of (5.5) ensures that discrete analogues of the integrated conservation laws are satisfied at convergence, with the boundary conditions determining how well the boundary fluxes are approximated. Clearly K should be invertible so that the complete system of conservation laws holds. This lemma obviously does not give the most general allowable condition, since we may allow the bracketed terms of the update equation (5.2) to be premultiplied by any non-singular matrix $\{C_j\}$; the convergence of the updates then implies (5.5).

5.2. Convergence Analysis

The conditions needed for convergence are usually studied by Fourier analysis, but this requires rather restrictive assumptions on the Lax–Wendroff iteration. We wish to apply it to nonlinear equations on a nonuniform mesh and to choose local time steps, all conditions which lie out-

side a Fourier approach. We shall give the results from a Fourier analysis in Section 5.3 below, but we give here a result based on an energy analysis for the case of a scalar homogeneous equation.

Define the iteration error E_j^n and average wave speed \bar{a}_j^n by

$$E_j^n := W_j^n - W_j^\infty, \quad \bar{a}_j^n E_j^n := f(W_j^n) - f(W_j^\infty). \quad (5.6)$$

We introduce two global CFL parameters v_N and v_C , based on the nodes and the cells, respectively, in terms of which we can give the local nodal and cell time steps:

$$\Delta t_j = v_N \frac{h_{j-1/2} + h_{j+1/2}}{2|a_j^n|}, \quad \Delta t_{j-1/2} = v_C \frac{h_{j-1/2}}{|\bar{a}_{j-1/2}^n|}. \quad (5.7)$$

Note that \bar{a}_j^n in (5.6) is a time average while $\bar{a}_{j-1/2}^n$ in (5.7) is a space average; note too that the distribution matrices reduce to $1 \pm v_C \text{sign}(\bar{a}_{j-1/2}^n)$ so that (5.2), (5.3) reduce to

$$\begin{aligned} \delta W_j = & -\frac{v_N}{2|a_j^n|} \{ [1 + v_C \text{sign}(\bar{a}_{j-1/2}^n)] h_{j-1/2} R_{j-1/2} \\ & + [1 - v_C \text{sign}(\bar{a}_{j+1/2}^n)] h_{j+1/2} R_{j+1/2} \}. \end{aligned} \quad (5.8)$$

Then subtracting equilibrium relations from the update equation we have

$$\begin{aligned} E_j^{n+1} = & E_j^n - \frac{v_N}{2|a_j^n|} \{ [1 + v_C \text{sign}(\bar{a}_{j-1/2}^n)] \Delta_- (\bar{a}E)_j^n \\ & + [1 - v_C \text{sign}(\bar{a}_{j+1/2}^n)] \Delta_+ (\bar{a}E)_j^n \}, \end{aligned} \quad (5.9)$$

where we have used the standard forward and backward difference notation $\Delta_+ u_j := u_{j+1} - u_j$, $\Delta_- u_j := u_j - u_{j-1}$.

There are two main technical difficulties in the analysis, one stemming from the variable coefficients a , \bar{a} , and \tilde{a} , and the other arising from the boundary conditions. We anticipate that the Lax–Wendroff procedure will need to be modified for sonic points and shocks, so we minimise the first difficulty by assuming that all coefficients have the same sign, namely positive. Hence we assume that W_0^n is prescribed and therefore $E_0^n = 0$; and on the right we use the standard Lax–Wendroff condition that $f(W_N^n) = f(W_{N-1}^n)$ and, hence, that $E_N^n = E_{N-1}^n$. These conditions will lead to reasonably simple boundary terms in the analysis, for which we introduce the (time level dependent) weighted inner product

$$\langle u, v \rangle_a := \sum_{j=1}^{N-1} (\bar{a}_j^n a_j^n) u_j v_j \quad (5.10)$$

and its associated norm $\|u\|_a^2 := \langle u, u \rangle_a$.

THEOREM 5.2. *For the scalar homogeneous equation, with positive wave speeds and the solution prescribed on the left boundary, the Lax–Wendroff update on an arbitrary mesh with local time steps given by (5.7), and with zero extrapolated residual on the right boundary, satisfies*

$$\|E^{n+1}\|_a \leq \gamma \|E^n\|_a \quad \text{with } \gamma < 1, \quad (5.11)$$

if the CFL numbers satisfy

$$\begin{aligned} & \max(v_N/v_C, v_N v_C) \\ & < \sum_{j=1}^{N-1} [\Delta_- (\bar{a}_j^n E_j^n)]^2 \Big/ \sum_{j=1}^{N-1} [(\bar{a}_j^n/a_j^n) \Delta_- (\bar{a}_j^n E_j^n)]^2. \end{aligned} \quad (5.12)$$

Proof. Multiply (5.9) by $(\bar{a}_j^n a_j^n)^{1/2}$, square both sides, and sum over $j = 1, 2, \dots, N-1$ to obtain

$$\begin{aligned} \|E^{n+1}\|_a^2 = & \|E^n\|_a^2 + \frac{v_N^2}{4} \left[(1 - v_C)^2 \left\| \frac{\Delta_+ (\bar{a}^n E^n)}{a^n} \right\|_a^2 \right. \\ & \left. + (1 + v_C)^2 \left\| \frac{\Delta_- (\bar{a}^n E^n)}{a^n} \right\|_a^2 \right] \\ & - v_N \left\langle E^n, \frac{\Delta_+ (\bar{a}^n E^n) + \Delta_- (\bar{a}^n E^n)}{a^n} \right\rangle_a \\ & + v_N v_C \left\langle E^n, \frac{\Delta_+ (\bar{a}^n E^n) - \Delta_- (\bar{a}^n E^n)}{a^n} \right\rangle_a \\ & + \frac{1}{2} v_N^2 (1 - v_C^2) \left\langle \frac{\Delta_+ (\bar{a}^n E^n)}{a^n}, \Delta_- \frac{\bar{a}^n E^n}{a^n} \right\rangle_a. \end{aligned} \quad (5.13)$$

Summing the first inner product by parts yields a typical term

$$\bar{a}_j^n a_j^n E_j^n \left(\frac{\bar{a}_{j+1}^n E_{j+1}^n}{a_j^n} \right) - \bar{a}_{j+1}^n a_{j+1}^n E_{j+1}^n \left(\frac{\bar{a}_j^n E_j^n}{a_{j+1}^n} \right) = 0,$$

and the boundary conditions result in the relation

$$\left\langle E^n, \frac{\Delta_+ (\bar{a}^n E^n) + \Delta_- (\bar{a}^n E^n)}{a^n} \right\rangle_a = (\bar{a}_{N-1}^n E_{N-1}^n)^2. \quad (5.14)$$

Similarly, the second inner product reduces to

$$\begin{aligned} & \left\langle E^n, \frac{\Delta_+ (\bar{a}^n E^n) - \Delta_- (\bar{a}^n E^n)}{a^n} \right\rangle_a \\ & = - \sum_{j=1}^{N-1} [\Delta_- (\bar{a}_j^n E_j^n)]^2 \\ & =: - \|\Delta_- (\bar{a}^n E^n)\|_a^2. \end{aligned} \quad (5.15)$$

For the full inner product we must add to the Fourier analysis. The result is that

identities

$$2\langle u, v \rangle_a = (\|u\|_a^2 + \|v\|_a^2) - \|u - v\|_a^2 \quad (5.16a)$$

$$= -(\|u\|_a^2 + \|v\|_a^2) + \|u + v\|_a^2, \quad (5.16b)$$

according to whether $v_C \leq 1$ or $v_C \geq 1$. In the former case, combining these relations and neglecting the last term of (5.16a) gives

$$\begin{aligned} \|E^{n+1}\|_a^2 &\leq \|E^n\|_a^2 + \frac{v_N^2}{2} \left[(1 - v_C) \left\| \frac{\mathcal{A}_+(\bar{a}^n E^n)}{a^n} \right\|_a^2 \right. \\ &\quad \left. + (1 + v_C) \left\| \frac{\mathcal{A}_-(\bar{a}^n E^n)}{a^n} \right\|_a^2 \right] \\ &\quad - v_N v_C \|\mathcal{A}_-(\bar{a}^n E^n)\|_2^2, \end{aligned} \quad (5.17)$$

which can be further reduced, because the \mathcal{A}_+ norm is dominated by the \mathcal{A}_- norm, to

$$\|E^{n+1}\|_a^2 \leq \|E^n\|_a^2 + v_N \left[v_N \left\| \frac{\mathcal{A}_-(\bar{a}^n E^n)}{a^n} \right\|_a^2 \right]$$

generalisation of the iteration that has been made for an arbitrary mesh, and with two local time steps, is correct and exacts no significant convergence penalties.

5.3. Choice of CFL Parameters

A Fourier analysis of the constant coefficient linear advection equation gives the amplification factor

$$\lambda = 1 - iv_N \sin k \Delta x - 2v_N v_C \sin^2 \frac{1}{2} k \Delta x, \quad (5.22)$$

from which we deduce that

$$\arg \lambda = -\tan^{-1} \left[\frac{v_N \sin k \Delta x}{1 - 2v_N v_C \sin^2 \frac{1}{2} k \Delta x} \right], \quad (5.23)$$

$$\begin{aligned} |\lambda|^2 &= 1 - 4v_N \sin^2 \frac{1}{2} k \Delta x [(v_C - v_N) \\ &\quad + v_N(1 - v_C^2) \sin^2 \frac{1}{2} k \Delta x]. \end{aligned} \quad (5.24)$$

The stability conditions $v_N \leq v_C$ and $v_N v_C \leq 1$, corresponding to (5.12), follow immediately from (5.24). Moreover, it is clear from (5.23) that v_N largely determines the

$w(-1)=9$ chosen so that the solution is everywhere positive. The table shows the number of iterations required to drive the residuals to 10^{-9} , on a mesh of 50 nodes with constant initial data. The superiority of the upwind scheme over any other choice of the CFL parameters is most marked.

The same problem but with boundary data $w(-1)=9.0$, $w(+1)=-9.26$ gives a shocked solution. As remarked earlier, it is now not possible to set all the cell residuals to zero and the Lax-Wendroff iteration will pick out an approximation in which pairwise averages of residuals are set to zero. If the shock position is such that $\tilde{a}_{s-1/2} > 0$ and $\tilde{a}_{s+1/2} < 0$, then at convergence (5.8) reduces to

$$\begin{aligned} (1 + v_C) h_{j-1/2} R_{j-1/2} + (1 - v_C) h_{j+1/2} R_{j+1/2} \\ = 0, \quad j < s, \end{aligned} \tag{5.25a}$$

$$\begin{aligned} (1 + v_C)(h_{s-1/2} R_{s-1/2} + h_{s+1/2} R_{s+1/2}) \\ = 0, \quad j = s, \end{aligned} \tag{5.25b}$$

$$\begin{aligned} (1 - v_C) h_{j-1/2} R_{j-1/2} + (1 + v_C) h_{j+1/2} R_{j+1/2} \\ = 0, \quad j > s. \end{aligned} \tag{5.25c}$$

Thus (5.25b) shows that the residuals that straddle the shock have opposite signs; (5.25a) and (5.25c) combine to show that there is a decay of residuals away from the shock, the decay being monotone if $v_C > 1$, oscillatory if $v_C < 1$, and immediate if $v_C = 1$. Only in the last case are the residuals other than $R_{s-1/2}$ and $R_{s+1/2}$ set to zero, the transition being sharp with just two "shock cells." This is the motivation for using upwind distribution matrices, tuned to the shock wave, which will be discussed in the next section. It is worth noting that, if v_C is based on the wave speed $\tilde{a} = \Delta f / \Delta W$, then for homogeneous problems $v_C \geq 1$ ensures that the updates are TVD.

Figure 3a shows a typical result obtained with $v_C = 2.0$, $v_N = 0.5$. It will be noted that the position of the shock is not very accurate: this is partly because the trapezoidal rule

used in (3.2) to calculate the residual has a large error for the cell containing a shock; and also because (5.25b) gives a poorly conditioned equation for W_s , since the dependence on W_s is only through the inhomogeneous term. The introduction of some second-order artificial viscosity in just this equation to force W_s close to $\frac{1}{2}(W_{s-1} + W_{s+1})$ can alleviate both of these problems, as W_{s-1} and W_{s+1} are well defined by the other equations.

By imposing no boundary data and replacing the forcing function by $g(x, w) = \frac{1}{2}\pi \sin \pi x$, we obtain a transcritical expansion for the exact solution of the inviscid Burgers' equation. The results obtained with the same choice of CFL parameters, and with initial data such that $W_0^0 < 0$ and $W_N^0 > 0$, is shown in Fig. 3b. The discrete solution with a spurious expansion shock is typical of all choices of CFL parameters. The system of residual equations is now underdetermined and the solution obtained depends on the initial data and the choice of v_C ; indeed, the expansion point value W_e^n , for which $\tilde{a}_{e-1/2} < 0$ and $\tilde{a}_{e+1/2} > 0$, is never changed for the upwind choice $v_C = 1$. With the Lax-Wendroff method this situation can only be avoided by the use of artificial viscosity terms; in practical multidimensional calculations such as in [1] this is provided by the fourth-order artificial viscosity.

5.4. Application to the de Laval nozzle problem

For a system of equations, such as the isenthalpic Euler equations of (2.3), the local time steps have to be based on the maximum characteristic speed $|\lambda^{\max}|$ of the Jacobian matrix A . Thus in terms of global CFL parameters v_N and v_C , we use the cell-averaged Jacobians \tilde{A} to replace (5.7) by

$$\begin{aligned} \Delta t_{j-1/2} &= v_C \frac{h_{j-1/2}}{|\tilde{\lambda}_{j-1/2}^{\max}|}, \\ \Delta t_j &= \frac{v_N}{v_C} \min(\Delta t_{j-1/2}, \Delta t_{j+1/2}). \end{aligned} \tag{5.26}$$

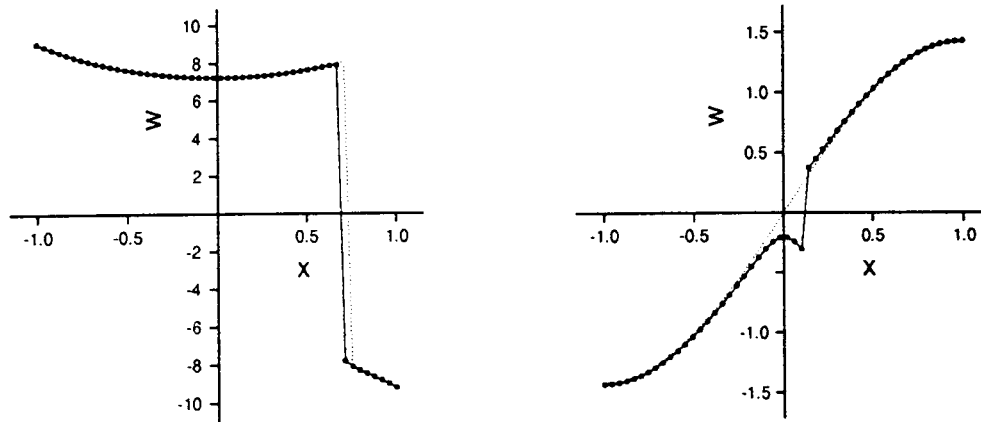


FIG. 3. Discrete solutions of the inviscid Burgers' equation: (a) with a shock; (b) with a transcritical expansion, obtained with the Lax-Wendroff update. In both cases $v_N = 0.5$, $v_C = 2.0$ and the exact solution is shown as a dotted line.

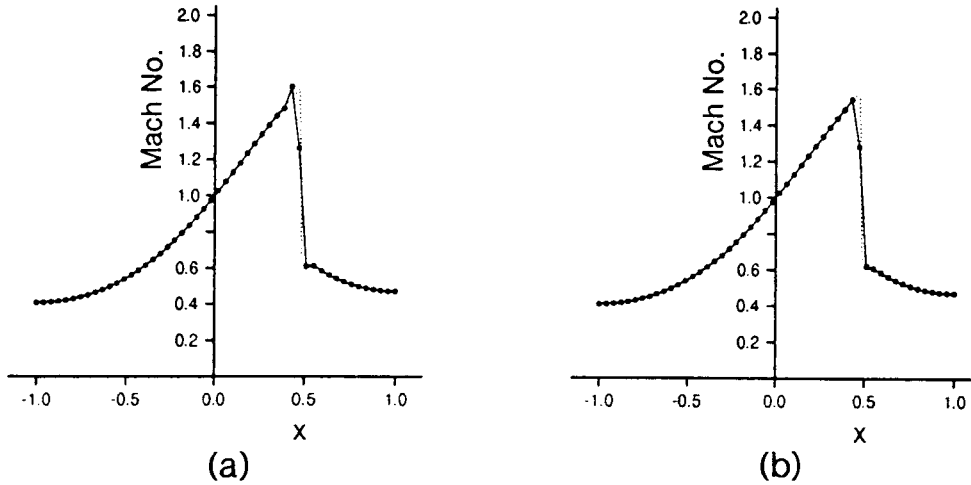


FIG. 4. Discrete solutions for transcritical flow in a de Laval nozzle with $M_\infty = 0.5$ obtained with the generalised Lax–Wendroff scheme: (a) $v_N = 0.25$, $v_C = 4.0$; (b) $v_N = 0.16$, $v_C = 6.0$.

However, in the scalar case we have seen that taking $v_C = 1$, corresponding to simple upwinding, has several advantages; so here we might impose “selective upwinding” by choosing v_C locally to correspond to upwinding for a particular wave mode, i.e., for the mode $\tilde{\lambda}^{(i)}$ we set

$$(v_C)_{j-1/2} = \frac{|\tilde{\lambda}_{j-1/2}^{(\max)}|}{|\tilde{\lambda}_{j-1/2}^{(i)}|}, \quad (5.27)$$

although an upper limit might be placed on this should the wave speed of the selected mode approach zero. This idea will be exploited more in the next section.

Let us consider a transonic nozzle problem with subsonic inlet and outlet conditions and cross-sectional area given by (2.6). One physical boundary condition has to be imposed at each boundary, while the Lax–Wendroff algorithm requires all boundary values to be updated. This is achieved in two stages: in the first, the Lax–Wendroff update is applied to the complete vector of unknowns at each boundary by setting a fictitious external residual equal to zero; then the change to the incoming characteristic variable is approximately set to zero by corrected updates obtained from setting $\mathbf{I}_0^{(+)} \delta \mathbf{W}_0^c = 0$ and $\mathbf{I}_N^{(-)} \delta \mathbf{W}_N^c = 0$, where $\mathbf{I}_0^{(+)}$ is the (rectangular) matrix of left eigenvectors of A_0 corresponding to positive (i.e., incoming) eigenvalues and $\mathbf{I}_N^{(-)}$ is similarly defined. Initial conditions are assumed to be constant and consistent with the boundary data.

Setting $M_\infty = 0.4$ as in the first example of Section 4 gives a subcritical flow and, on a uniform mesh of fifty nodes, all the cell residuals can be driven to 10^{-9} by using (5.2) with $v_N v_C = 1$; as in the scalar case the choice $v_C = 1$ is best, taking some 1500 iterations, with other choices taking a number of steps roughly proportional to v_C .

However, for all supercritical cases, where a sonic point (at $x = 0$) and a shock appear, the cell residuals cannot be

driven to zero in their neighbourhoods. Convergence of the iteration is therefore based on the scaled nodal residuals $\delta \mathbf{W}_j / \Delta t_j$. No steady state can be reached, even on this basis for the standard Lax–Wendroff algorithm ($v_C = v_N$) unless some artificial viscosity is added. But for $v_C = 6$ and $M_\infty = 0.5$ the nodal residuals can be driven to 10^{-8} in about 10,000 iterations, after which updates of this order persist in the neighbourhood of the sonic point. The results for two choices of the CFL parameters are shown in Fig. 4; for smaller values of v_C an expansion shock appears at the sonic point, and for larger values the shock is smeared and convergence is slower. Very similar results can be obtained by adding artificial viscosity to the standard Lax–Wendroff scheme with only some 2000 iterations; rather sharper results can be obtained using the selected upwinding scheme (5.27) based on the slower wave speed, but some 50,000 iterations are required.

In summary, then, the generalised Lax–Wendroff scheme can be used to obtain steady solutions to this model problem, but ignoring the counting problems at the sonic point and the shock exacts a heavy penalty in the rate of convergence achieved. The CFL parameters can be generalised further to yield a “matrix time-stepping” scheme; such developments lead naturally to the schemes considered in the next section.

6. GENERAL UPWIND ITERATION SCHEMES

In the previous section we discussed the use of generalised Lax–Wendroff time-stepping schemes and their effect on the discrete solution in the region of sonic points and shock waves. We have also examined marching procedures aimed at solving the cell vertex equations in a more efficient and direct manner. Here we shall attempt to combine the two

techniques in order to obtain the best possible solution with the minimum of effort, for both subcritical and supercritical cases.

The general class of problems to which we wish to apply the methods is of the form

$$(\mathbf{f}(\mathbf{w}, \mathbf{w}_x))_x = \mathbf{g}(x, \mathbf{w}), \quad (6.1)$$

from which we can construct cell residuals $\mathbf{R}_{j-1/2}$ using (3.2), (3.4), and (3.5); note, however, that the Jacobian is always calculated as $A := \partial \mathbf{f} / \partial \mathbf{w}$.

6.1. Nodal Residual Mappings

As mentioned in the Introduction, one of the characteristic features of the cell-vertex method is the lack of a natural correspondence between cell residuals and nodal

\mathbf{w} . Typically then, if the cell residuals involve both viscous and inviscid terms, it is the inviscid terms which influence their distribution. The above approach to generalisation of the scalar upwind mapping is equivalent to introducing a cell-based matrix time-step—i.e., introducing a cell time step *for each wave mode*. Introducing the notation $\text{sign}(A) = V \text{sign}(A) V^{-1}$, Eq. (6.3) can be written more concisely as

$$D_{j-1/2}^{\pm} = I \pm \text{sign}(\tilde{A}_{j-1/2}). \quad (6.4)$$

Having defined the mapping (6.2) from cell to nodes, the solution is obtained by setting $\mathbf{N}_j = 0$ at each node, subject to suitable boundary conditions. An advantage of the upwind distribution matrices is that the non-reflective boundary conditions of Section 5.4 can be implemented in a very natural and straightforward manner. This is achieved

The definition of the local relaxation parameter ω_j depends on the spectral radii of the local Jacobian matrices. The most common choice is

$$\omega_j = v \max \left(\frac{h_{j+1/2}}{\rho(\tilde{A}_{j+1/2})}, \frac{h_{j-1/2}}{\rho(\tilde{A}_{j-1/2})} \right), \quad (6.8)$$

with $\rho(A)$ denoting the spectral radius of A and $v \in (0, 1)$ is the usual CFL parameter. Such a scheme, i.e., based on (6.4), (6.7), and (6.8), was originally used by Huang [7] and was conceived as a generalisation to steady-state problems of the earlier work by Steger and Warming [19]. For a particular choice of the cell quantity \tilde{A} deduced from the linearisation $\Delta \mathbf{f} = \tilde{A} \Delta \mathbf{W}$, it is simple to show that this scheme is equivalent to that proposed by Roe [17].

We have already observed in Section 6.1 that the generalised upwind distribution matrices (6.4) may be obtained from the Lax–Wendroff distribution matrices by introducing a cell-based matrix time step. It is therefore also natural to define the nodal time step as a matrix; or equivalently to let the relaxation parameter in (6.7) assume matrix values. With reference to the scalar time step defined in (5.7), the update becomes

$$\delta \mathbf{W}_j = -\frac{1}{2} |A_j|^{-1} (D_{j-1/2}^+ h_{j-1/2} \mathbf{R}_{j-1/2} + D_{j+1/2}^- h_{j+1/2} \mathbf{R}_{j+1/2}), \quad (6.9)$$

where $|A_j| = V_j |A_j| V_j^{-1}$, analogous to the definition of $\text{sign}(\tilde{A})$. The update is then the true vector counterpart of the scalar upwinding scheme. This matrix time step may be viewed as a means of normalising the speed of each wave independently and the technique may thus be expected to give improvements over the nodal time step of (5.27) as the ratio of the speeds of fastest and slowest wave increases—see [22] for a similar algorithm.

Consider now the application of a nonlinear variant of the Jacobi method to the system $\mathbf{N}_j = 0$, $j = 0, \dots, N$. As applied to linear problems, an iteration of Jacobi adjusts the unknowns at each given node to set the corresponding residuals to zero. Residuals are calculated using only solution values from the previous iteration. For nonlinear problems the same principle can be applied by using Newton's method to solve the local nonlinear problem $\mathbf{N}_j = 0$ for each j . In practice the Newton iterations may be discontinued before the local problem has converged. A single iteration of Newton's method gives the update

$$\delta \mathbf{W}_j = -\frac{\mathcal{A}_j^{-1}}{h_{j-1/2} + h_{j+1/2}} (D_{j-1/2}^+ h_{j-1/2} \mathbf{R}_{j-1/2} + D_{j+1/2}^- h_{j+1/2} \mathbf{R}_{j+1/2}), \quad (6.10)$$

where the Jacobian of the nodal residual is defined as $\mathcal{A}_j :=$

$\partial \mathbf{N}_j / \partial \mathbf{W}_j$. Moreover, if we assume that we use the upwind distribution matrices (6.4) in (6.10) and that they are independent of \mathbf{W}_j , this iteration reduces to

$$\delta \mathbf{W}_j = -\frac{1}{2} (\bar{A}_j)^{-1} [(I + \text{sign}(\tilde{A}_{j-1/2})) h_{j-1/2} \mathbf{R}_{j-1/2} + (I - \text{sign}(\tilde{A}_{j+1/2})) h_{j+1/2} \mathbf{R}_{j+1/2}], \quad (6.11)$$

where

$$\begin{aligned} \bar{A}_j &= \frac{1}{2} (\text{sign}(\tilde{A}_{j-1/2}) + \text{sign}(\tilde{A}_{j+1/2})) A_j \\ &\quad - \frac{1}{2} \{ (I + \text{sign}(\tilde{A}_{j-1/2})) h_{j-1/2} \\ &\quad + (I - \text{sign}(\tilde{A}_{j+1/2})) h_{j+1/2} \} B_j, \end{aligned} \quad (6.12)$$

with $B_j = (\partial \mathbf{g} / \partial \mathbf{w})_j$. Noting that $\text{sign}(A) A = |A|$, we see that this scheme closely resembles the matrix time stepping scheme (6.9); the difference is more marked near sonic points where the matrix \bar{A}_j will need to be modified. The treatment of such critical points and their effect on the iteration will be discussed in detail in Section 6.3, although it is worth noting here that there appears to be no practical advantage of using (6.11) rather than the simpler (6.9).

A simple variant of this scheme or that based on (6.9), which is derived from the Jacobi method, is to base them on the Gauss–Seidel scheme, in which the nodes are updated sequentially using the latest values to evaluate \mathbf{N}_j . When the local iteration is continued until the nodal residuals are set to zero, we call this the *general marching scheme*. In the scalar case, with a constant wave direction, such an algorithm is very efficient if we update the \mathbf{W}_j sequentially in the direction of the wavespeed, since away from critical points the nodal residual \mathbf{N}_j depends only on discrete values at the adjacent upstream node, as well as the node j itself. Various orderings of the nodes are possible for Gauss–Seidel; it can converge fast when marched downstream but generally behaves like Jacobi when it is marched upstream. In the case where the Jacobian has eigenvalues of opposite signs it is therefore advisable to use the symmetric Gauss–Seidel, which visits the nodes first from left to right, and then in reverse order.

The symmetric Gauss–Seidel iteration applied to the nodal equations (6.2), with upwind distribution matrices defined by (6.4) is closely related to the special marching scheme discussed in Section 4.1. The rank of the upwind distribution matrices is such that the nodal residual automatically receives the correct amount of information from each neighbouring cell. For the subcritical nozzle problem the convergence behaviour of the two methods is very similar. The advantage of the upwinding approach is in its treatment of critical points, which allows shocks to be captured in the correct location, without significant modification to the algorithm.

In order to compare the efficiency of the present upwind

iteration schemes with that of the simple marching scheme of Section 4, we present results for the subsonic test case, with $M_\infty = 0.4$. Table III shows the number of iterations required by various techniques to reduce the l_2 norm of the nodal residuals to 10^{-9} , on a regular grid of N points; optimal relaxation parameters are used in each case and for the symmetric Gauss-Seidel and marching the number of single sweeps is given. We note that the matrix time-stepping method (6.9) requires between a third and a quarter of the iterations required by its standard counterpart (6.7), this being inversely proportional to the grid spacing in both cases. Such an improvement is to be expected, since the ratio of the convergence rates would be better than $|\lambda^{(2)}| : |\lambda^{(1)}|$ for a linear problem—for the range of Mach numbers 0.4 to 0.8 this quantity takes values from approximately 2:1 to 9:1. Although the update (6.9) is more expensive to compute, the extra work is minimal for our two by two system. However, the computational cost would become a more important factor for larger systems of equations.

As expected, the schemes based on the use of the symmetric Gauss-Seidel give vast improvements over the point iteration methods. With just one iteration at each point, the SGSM scheme gives a sevenfold improvement at $N = 17$ and this increases with N ; the general marching scheme gives further improvement and is fully grid-independent. The use of (6.9) either for a single iteration or for driving the nodal residuals to zero, as in the marching scheme, is as effective as using the Newton iteration (6.10), (6.11). The number of iterations required at each node was typically less than eight, with fewer needed on the finer grids, so that GM is much more efficient than SGSM.

6.3. Application to the Transonic Nozzle Problem

As we saw with the simple marching schemes in Section 4.2, the above techniques require further modification before they can be expected to give reliable solutions of the transonic nozzle problem. This is because the local counting problem regarding the cell residuals at sonic points exhibits itself in the nodal residuals as near-singularities in the

Jacobian matrices, or loss of linear independence of the nodal equations. We therefore use modifications similar to those in Section 4.2.

We begin by considering the scalar problem, denote the position of the critical point as x_c , and define the interval $(k, k + 1)$ such that $a_k < 0 < a_{k+1}$. Linear interpolation of the wavespeed a gives

$$\theta_c \approx -\frac{a_k}{\Delta a_{k+1/2}}, \tag{6.13}$$

where θ_c represents the ratio $(x_c - x_k) : (x_{k+1} - x_k)$. We define two “partial” residuals $R_{k+1/2}^-$ and $R_{k+1/2}^+$ and, in order to avoid limit cycles as θ_c tends to 0 or 1, use the full interval length in calculating the nodal residuals

$$\begin{aligned} N_k &= \frac{h_{k+1/2}}{h_{k-1/2} + h_{k+1/2}} R_{k+1/2}^- \\ &= \frac{h_{k+1/2}}{h_{k-1/2} + h_{k+1/2}} \left[\frac{f(w_c) - f_k}{\theta_c h_{k+1/2}} - \frac{1}{2} (g_k + g_c) \right] \\ N_{k+1} &= \frac{h_{k+1/2}}{h_{k+1/2} + h_{k+3/2}} R_{k+1/2}^+ \\ &= \frac{h_{k+1/2}}{h_{k+1/2} + h_{k+3/2}} \left[\frac{f_{k+1} - f(w_c)}{(1 - \theta_c) h_{k+1/2}} - \frac{1}{2} (g_c + g_{k+1}) \right]. \end{aligned} \tag{6.14}$$

This may be modified in several ways. We may, for example, make explicit use of the approximation

$$\begin{aligned} f(w_c) - f_k &\approx \frac{1}{2} a_k (w_c - W_k) \\ &\approx \frac{1}{2} (W_k - w_c) \theta_c h_{k+1/2} \Delta a_{k+1/2}, \end{aligned} \tag{6.15}$$

with a similar expression for $f_{k+1} - f_c$. The values of $w(x_c)$ and $g(w(x_c), x_c)$ may also be estimated by assuming that w and g vary linearly within the interval, instead of assuming sonic conditions there. The latter approach is essentially that taken by van Leer *et al.* [21], who describe a generalisation to inhomogeneous equations of the “entropy fix” proposed by Harten [6]. It may also be shown that the present method is a generalisation of that of Roe [20]. Finally, we note that whilst the weighted sum of the residuals approximates a residual for the complete cell, the difference $R_{k+1/2}^+ - R_{k+1/2}^-$ may be thought of as an approximation to the derivative of the steady differential equation (2.1) evaluated at w_c, x_c , where $a(w_c) = 0$. We note that this difference may be used directly to augment the original system of cell residuals, without defining the partial residuals.

The generalisation of these ideas to the transonic nozzle problem is straightforward. Consider a sonic point corresponding to the eigenvalue $\lambda^{(1)}$ and let us assume that the left eigenvector $\mathbf{I}^{(1)}$ is constant in its neighbourhood. We

TABLE III

Convergence Behaviour for the Subsonic Problem

N	T-S	M-T-S	S-G-S-M	G-M
17	571	163	22	8
33	1108	310	27	8
65	2155	601	33	8
129	4234	1184	57	8
257	8387	2351	93	7

Note. T-S = time-stepping by (6.7); M-T-S = matrix time-stepping by (6.9); S-G-S-M = symmetric Gauss-Seidel using the matrix parameter of (6.9); G-M = general marching with symmetric Gauss-Seidel and (6.9).

TABLE IV

Convergence Behaviour for the Transonic Problem

N	T-S	M-T-S	S-G-S-M	G-M
17	601	87	37	14
33	1385	184	82	*
65	2590	301	130	15
129	4934	787	312	15
257	9912	1362	561	14

Note. T-S = time-stepping by (6.7); M-T-S = matrix time-stepping by (6.9); S-G-S-M = symmetric Gauss-Seidel using the matrix parameter of (6.9); G-M = general marching with symmetric Gauss-Seidel and (6.9), with residuals modified by (6.17) in each case.

(6.9) must be modified to avoid the smallest eigenvalue of $|A|$ from tending to zero; in practice, we may replace λ_j by $\max(|\tilde{\lambda}_{j-1/2}|, |\tilde{\lambda}_{j+1/2}|)$ and impose lower limits on its size. This difficulty is avoided by using the Jacobi-Newton technique (6.10) if the Jacobian matrix is calculated directly from (6.17). However, we have found this latter technique to be unreliable at both the sonic point and the shock transition node. Finally, we note that the general marching scheme may be improved by solving the two nodal equations adjacent to the sonic point *simultaneously* during each sweep.

Table IV shows convergence results of a transonic test case, with $M_\infty = 0.5$, for various iteration techniques. In comparison with the subcritical results, matrix time-stepping gives even greater gains over the scalar time step (note that the ratio $|\lambda^{(2)}| : |\lambda^{(1)}|$ becomes extremely large close to the sonic point). Once again, the general marching algorithm is the most efficient technique, although its convergence behaviour is somewhat worse than that of the subcritical problem due to the (relatively) slow convergence of the shock transition node. In going from matrix time-stepping to general marching, the change to the symmetric Gauss-Seidel gives only moderate gains while the iteration to local convergence gives the greatest gains. Although the definition of a simultaneous iteration for the nodal equations bracketing the sonic point is important for the smooth evolution of the solution, it was not found to improve the global convergence noticeably. However, this would seem to depend on the choice of initial conditions, the modification being crucial in the scalar case. Figure 5a shows a Mach number distribution obtained with just one double sweep (note that the sonic point has already settled at the throat of the nozzle); Fig. 5b shows the solution a double sweep later; the converged solution is given in Fig. 5c. Finally, Fig. 5d shows the converged solutions obtained without any modification to take account of the sonic point, demonstrating the occurrence of an unphysical expansion shock.

7. CONCLUSIONS

As used successfully for the Navier-Stokes equations in two and three dimensions, the cell vertex method described in [1] has four main components—definition of the cell residuals \mathbf{R}_x , use of distribution matrices $D_{x,j}$ to form nodal residuals \mathbf{N}_j , addition of second- and fourth-order artificial viscosity, and pseudo time-stepping to steady state with multigrid acceleration. Specialisation of this method to the one-dimensional model problems (2.3) and (2.7) has formed the starting point of the present study, which has then gone on to see how far and by what means the scheme can be improved. The outcome is shown by the results quoted in Section 5.4 and those summarised in Table III and Table IV, which show vast improvements and culminate in highly effective schemes while still staying in the same basic framework.

It is notoriously difficult to translate algorithmic improvements in one dimension to two and three dimensions, but here we will speculate on the prospects in the present case. Our first step was to use the upwind distribution matrices (6.4) instead of the Lax-Wendroff matrices of (5.3); for a scalar problem in 2D this entails switching from $1 \pm v_C^{(x)} \pm v_C^{(y)}$ which is the standard generalisation of the terms in (5.8), to $(1 \pm v_C^{(x)})(1 \pm v_C^{(y)})$ with $|v_C^{(x)}| = |v_C^{(y)}| = 1$, so that only one cell contributes to the update at a vertex, instead of all four of those that meet there. For the cell vertex residuals, a Fourier analysis shows that instead of the stability condition $v_C v_N < 1$ one then finds that no choice of v_N is stable; that is, the first two columns of Tables III and IV become infinite! Yet one can show that this is overcome by the next step of using the Gauss-Seidel techniques, which give the third columns in the tables; so, for example, the slow convergence of Lax-Wendroff (and the poor quality of converged solution) can be completely overcome for 2D convection-diffusion problems by the steps described in this paper.

A key generalisation is then to systems of equations. When the steady system is hyperbolic, as for flow which is everywhere supersonic so that streamlines define a time-like direction, experience with space marching schemes suggest that there will be no particularly significant problems. Major difficulties occur, however, when at least part of the flow is subsonic, giving a mixed elliptic/hyperbolic system. A relevant model problem is given by the Cauchy-Riemann equations, and how to set up and solve the cell vertex discretisation of these still needs much more study. Note that we have not had to use multigrid techniques in one dimension, but they will undoubtedly be needed here. Solving the Cauchy-Riemann problem and incorporating the result into the solution of the transonic flow problems seems to be the crucial step in taking the results of this paper into two dimensions. For consider the final stage in our sequence of iterative methods, namely local iteration; preliminary

experience suggest that using this in the fully supersonic inviscid case, by applying the present methods at each fixed x station, works well. It is again the transonic situation that requires the most attention.

REFERENCES

1. P. I. Crumpton, J. A. Mackenzie, and K. W. Morton, *J. Comput. Phys.* **109**, 1 (1993).
2. P. I. Crumpton, J. A. Mackenzie, and K. W. Morton, in *Thirteenth International Conference on Numerical Methods in Fluid Dynamics, Proceedings, Consiglio Nazionale delle Ricerche, Rome, Italy, July 1992*, edited by M. Napolitano and F. Sabetta. Lecture Notes in Physics, Vol. 414 (Springer-Verlag, New York/Berlin, 1993), p. 519.
3. P. I. Crumpton, J. A. Mackenzie, K. W. Morton, M. A. Rudgyard, and G. J. Shaw, in *Twelfth International Conference on Numerical Methods in Fluid Dynamics, Proceedings, University of Oxford, England, July 1990*, edited by K. W. Morton. Lecture Notes in Physics, Vol. 371 (Springer-Verlag, New York/Berlin, 1990), p. 243.
4. V. A. Gushchin and V. V. Shchennikov, *U.S.S.R. Comput. Math. Math. Phys.* **14**, 252 (1974).
5. M. G. Hall, in *Proceedings, Conference on Numerical Methods for Fluid Dynamics, University of Reading*, edited by K. W. Morton and M. J. Baines. (Oxford Univ. Press, London, 1985), p. 303.
6. A. Harten, *J. Comput. Phys.* **49**, 357 (1983).
7. L. C. Huang, *J. Comput. Phys.* **42**, 195 (1981).
8. J. E. Lavery, *J. Comput. Phys.* **79**, 436 (1988).
9. A. Lerat, *C.R. Acad. Sci. A* **288**, 1033 (1979).
10. H. Liepmann and A. Roshko, *Elements of Gas Dynamics* (Wiley, New York, 1957).
11. J. A. Mackenzie and K. W. Morton, *Math. Comput.* **60**, 189 (1992).
12. K. W. Morton, P. N. Childs, and M. A. Rudgyard, in *Proceedings, IMA Conference, Numerical Methods for Fluid Dynamics III*, edited by K. W. Morton and M. J. Baines (Oxford Univ. Press, Oxford, 1988), p. 137.
13. K. W. Morton, P. I. Crumpton, and J. A. Mackenzie, *Comput. Fluids* **22**, Nos. 2/3, 91 (1993).
14. K. W. Morton and M. F. Paisley, *J. Comput. Phys.* **80**, 168 (1989).
15. K. W. Morton and M. A. Rudgyard, in *Proceedings, 11th International Conference on Numerical Methods in Fluid Dynamics, Williamsburg, USA 1988*, edited by D. L. Dwoyer, M. Y. Hussaini, and R. G. Voigt. Lecture Notes in Physics, Vol. 323 (Springer-Verlag, New York/Berlin, 1989), p. 424.
16. R. H. Ni, *AIAA J.* **20**, 1565 (1982).
17. P. L. Roe, *Annu. Rev. Fluid Mech.* **18**, 337 (1986).
18. P. L. Roe and B. van Leer, in *Numerical Methods for Fluid Dynamics III*, edited by K. W. Morton and M. J. Baines (Oxford Univ. Press, Oxford, 1988), p. 520.
19. J. L. Steger and R. F. Warming, *J. Comput. Phys.* **40**, 263 (1981).
20. B. van Leer, *SIAM J. Sci. Stat. Comput.* **5**, No. 1, 1 (1984).
21. B. van Leer, W.-T. Lee, and K. G. Powell, AIAA Paper 89-45-CP, The University of Michigan, Department of Aerospace Engineering, 1989 (unpublished).